

Diamagnetic Ru^{2+} in $\text{Na}_2\text{La}_2\text{Ti}_2\text{RuO}_{10-x}$ ($0 < x < 2$): a series of complex oxides prepared by topochemical reduction.

*Jacob A. Pratt, Ashley M. Shepherd and Michael A. Hayward**

Department of Chemistry, University of Oxford, Inorganic Chemistry Laboratory, South Parks Road, Oxford, OX1 3QR, United Kingdom.

ABSTRACT

Reaction of the $n = 3$ Ruddlesden-Popper phase $\text{Na}_2\text{La}_2\text{Ti}_2\text{RuO}_{10}$ with a 5% H_2 / 95% N_2 atmosphere between 300 °C and 900 °C leads to the formation of phases of composition $\text{Na}_2\text{La}_2\text{Ti}_2\text{RuO}_{10-x}$ ($0 < x < 2$) via topochemical reduction. Magnetization data collected from $\text{Na}_2\text{La}_2\text{Ti}_2\text{RuO}_{10-x}$ samples in the range $0 < x < 1$ show a rapid decline in susceptibility with increasing x , consistent with the conversion of $S = 1$, Ru^{4+} centers at $x = 0$ to $S = 0$, Ru^{2+} centers at $x = 1$. We believe this is the first report of diamagnetic Ru^{2+} centers in an extended oxide phase. Further reduction of $\text{Na}_2\text{La}_2\text{Ti}_2\text{RuO}_9$ leads to the reduction of Ti^{4+} to Ti^{3+} , however $\text{Na}_2\text{La}_2\text{Ti}_2\text{RuO}_{10-x}$ samples in the range $1 < x < 2$ exhibit only a very weak paramagnetic response. Given the highly insulating nature of the phases, this suggests the electrons added on reduction of titanium are paired within a local Ti-Ti bonding network in a manner analogous to that observed for $\text{Ti}_n\text{O}_{2n-1}$ phases.

Introduction

Complex transition metal oxides have been the subject of extensive study due to the variety of electronic and magnetic properties they can exhibit, which include superconductivity, colossal magnetoresistance and broad range of other coupled transport and collective magnetic behavior.¹ These complex electronic behaviors arise from electrons located in partially-filled metal d-states which can couple to each other, either through the direct mixing of orbitals on neighboring metal centers, or via the orbitals of bridging ligands. The complex electronic states which emerge in these systems can therefore be considered to be a function of the identity, oxidation state and local coordination geometry of the transition metal centers, which together define local electronic states of the metal cations, and the structure and chemical makeup of the extended metal-anion network, which defines the nature and strength of inter-metal electronic coupling.

There has been growing interest in extended oxide phases containing more than one type of transition metal cation, with a particular focus on mixed 3d/4d and 3d/5d transition metal oxide systems where the energy difference between the relatively compact 3d orbitals and the more radially expanded 4d and 5d orbitals can modulate inter-cation coupling interactions and lead to complex electronic behavior. Such behavior is observed in the 3d/4d transition metal double perovskite oxide $\text{Sr}_2\text{FeMoO}_6$ which exhibits half-metallic ferromagnetic behavior due to the magnetic coupling between electrons in localized 3d⁵ iron states and those in delocalized bands derived from molybdenum 4d orbitals.²

Recently we have been investigating the effect of topochemical reduction – the removal of oxide ions in low-temperature structure conserving reactions – on mixed 3d/4d oxide systems. By using low-temperature synthesis methods the perovskite phase $\text{SrFe}_{0.5}\text{Ru}_{0.5}\text{O}_3$ can be reduced to $\text{SrFe}_{0.5}\text{Ru}_{0.5}\text{O}_2$ realizing Ru^{2+} centers in an extended oxide for the first time.^{3,4} Detailed

studies of this reduced phase have revealed that even though both the Fe^{2+} and Ru^{2+} cations are isoelectronic (d^6) and both are located in square-planar coordination environments, they adopt different spin states: Fe^{2+} $S = 2$, Ru^{2+} $S = 1$, further demonstrating the contrasting behavior of 3d and 4d transition metals.

Here we describe the topochemical reduction of the mixed 3d/4d Ruddlesden-Popper phase $\text{Na}_2\text{La}_2\text{Ti}_2\text{RuO}_{10}$. This phase was first reported by Lalena et al.⁵ to adopt an $n = 3$ Ruddlesden-Popper structure with strict $\text{La}^{3+}/\text{Na}^+$ cation order over the 12- and 9-coordinate A-cation sites, and partial $\text{Ti}^{4+}/\text{Ru}^{4+}$ order over the B-cation sites, as shown in Figure 1. The combination of partial B-cation order and weak electronic coupling between the ruthenium and titanium centers results in $\text{Na}_2\text{La}_2\text{Ti}_2\text{RuO}_{10}$ exhibiting insulating behavior with a magnetic response consistent with a spin-glass state, suggesting this phase is an example of a disordered Mott insulator. Introducing additional electrons into the metal d-states of the system, via topochemical reduction, allows the weak 3d/4d coupling to be investigated and parallels to the Fe/Ru system made.

Experimental

Samples of $\text{Na}_2\text{La}_2\text{Ti}_2\text{RuO}_{10}$ were prepared according to the method described by Lalena et al.⁵ Suitable stoichiometric ratios of La_2O_3 (99.999 %, dried at 900 °C), TiO_2 (99.995 %, dried at 900 °C) and RuO_2 (99.99%, dried at 800 °C) were combined with a 30% molar excess of anhydrous Na_2CO_3 (99.99%) in an agate pestle and mortar. After being ground into a homogenous powder, the mixture was then pressed into 13mm pellets under 5 tonnes force and heated at 1000 °C under flowing argon for 24 hours, prior to being washed with distilled water to remove any excess Na_2O , and then dried in air at 150 °C. A sample of $\text{Na}_2\text{La}_2\text{Ti}_3\text{O}_{10}$ was prepared by a similar method. X-ray powder diffraction data indicated that lattice parameters of

both $\text{Na}_2\text{La}_2\text{Ti}_2\text{RuO}_{10}$ and $\text{Na}_2\text{La}_2\text{Ti}_3\text{O}_{10}$ were in good agreement with previously reported values, and that $\text{Na}_2\text{La}_2\text{Ti}_2\text{RuO}_{10}$ samples had a partially ordered Ti/Ru distribution as reported previously.^{5,6}

$\text{Na}_2\text{La}_2\text{Ti}_2\text{RuO}_{10}$ samples were reduced by heating under a stream of 5% H_2 in N_2 at temperatures and for durations described in the text. ‘Reduced’ $\text{Na}_2\text{La}_2\text{Ti}_2\text{RuO}_{10-x}$ samples were treated as air-sensitive and handled in an argon filled glovebox ($p\text{O}_2$, $p\text{H}_2\text{O}$ < 1ppm), although there was no indication of rapid reoxidation of these samples at room temperature.

X-ray powder diffraction data were collected using a PANalytical X’pert diffractometer incorporating an X’celerator position-sensitive detector (monochromatic $\text{Cu K}\alpha_1$ radiation). Thermogravimetric reoxidation measurements were performed by heating powder samples at a rate of $5\text{ }^\circ\text{C min}^{-1}$ under oxygen using a Mettler-Toledo MX1 thermogravimetric microbalance. Magnetization data were collected from well ground samples as a function of temperature in an applied field of 100 Oe using a Quantum Design MPMS SQUID magnetometer. Resistivity measurements were performed using a 4-probe method on sample bars of known dimension cut from cold-pressed pellets. XPS data were collected using a VG Escalab Mk II spectrometer using Al $\text{K}\alpha$ X-rays (photon energy 1486.6 eV) and hemispherical analyzer for detection of electrons. Spectra were collected using a constant analyzer pass energy of 50 eV for survey scans and 20 eV for detailed scans. All spectra were referenced to the C1s peak using a binding energy of 285 eV.

Results

X-ray powder diffraction data collected from $\text{Na}_2\text{La}_2\text{Ti}_2\text{RuO}_{10}$ samples which had been heated in a 5% H_2 / 95% N_2 gas flow under conditions described in Table 1 could be indexed using body-centered tetragonal unit cells with lattice parameters also listed in Table 1. Rietveld

refinement of models based on the structure of $\text{Na}_2\text{La}_2\text{Ti}_2\text{RuO}_{10}$ gave good fits to the X-ray data indicating that the basic structure of the $\text{Na}_2\text{La}_2\text{Ti}_2\text{RuO}_{10-x}$ phases has been conserved during the reduction reaction (full details are given in the Supporting Information). The weak X-ray scattering power of oxygen, compared to the metals in the system, meant it was not possible to accurately locate the anion vacancies within the structures of the reduced phases, with the data suggesting the vacancies were distributed approximately evenly across all four anion sites. Thermogravimetric reoxidation of the samples back to $\text{Na}_2\text{La}_2\text{Ti}_2\text{RuO}_{10}$, under flowing oxygen (Figure 2) allowed their compositions to be determined as listed in Table 1. In combination, the X-ray diffraction data and TGA data confirm that a series of $\text{Na}_2\text{La}_2\text{Ti}_2\text{RuO}_{10-x}$ $0 < x < 2$ phases have been prepared via topochemical reduction. Attempts to reduce samples of $\text{Na}_2\text{La}_2\text{Ti}_3\text{O}_{10}$ under similar conditions were unsuccessful. Heating samples of $\text{Na}_2\text{La}_2\text{Ti}_3\text{O}_{10}$ to 950 °C on a thermogravimetric balance under a 5% H_2 in N_2 atmosphere resulted in no significant mass loss ($< 0.05\%$) and samples retained a white color after heating, indicating no oxygen loss had occurred.

Magnetization data collected from $\text{Na}_2\text{La}_2\text{Ti}_2\text{RuO}_{10}$ agree well with those previously reported by Lalena et al.,⁵ with zero-field cooled and field cooled data diverging for $T < 70$ K consistent with the reported spin-glass behavior of the phase. Analogous measurements performed on $\text{Na}_2\text{La}_2\text{Ti}_2\text{RuO}_{10-x}$ samples show no divergence between zero-field cooled and field cooled data in the measured temperature range, and as shown in Figure 3, the measured zero-field cooled magnetization decreases in magnitude and becomes less temperature dependent as the oxygen deficiency of samples increases. These features of the magnetization data can be quantified by fitting the Curie-Weiss law ($\chi = C/(T - \theta) + K$) to selected temperature ranges of the data as described in Table 2.

Resistivity measurements indicated that all $\text{Na}_2\text{La}_2\text{Ti}_2\text{RuO}_{10-x}$ samples are highly resistive at 300 K as shown in Figures 4 and 5. This high resistivity limited the temperature range over which transport measurements could be performed, however it could be determined that all samples exhibited semiconducting behavior ($dp/dT < 0$). Figure 4 shows data collected from $\text{Na}_2\text{La}_2\text{Ti}_2\text{RuO}_{9.23}$, which are typical of all samples. Fits to these data shown in the inset to Figure 4 indicate a $\ln\rho \propto T^{-1/4}$ temperature dependence consistent with the three-dimensional variable range hopping (VRH) of a small polaron conductor.

XPS data collected from $\text{Na}_2\text{La}_2\text{Ti}_2\text{RuO}_{10-x}$ samples in the energy range 275 – 295 eV, corresponding to the ionization energy of electrons in ruthenium 3d orbitals, show that the binding energies of both the Ru 3d_{5/2} (shown in Figure 5) and Ru 3d_{3/2} states (Supporting Information) decline with increasing x, consistent with the decline in the average ruthenium oxidation state. XPS data in the energy range 455-470 eV, corresponding to ionization from titanium 2p orbitals show the binding energy of Ti 2p_{3/2} and Ti 2p_{1/2} states changed by less than 0.2 eV over the whole compositional range. Given the surface sensitivity of the XPS technique, the invariance of the Ti binding energies is attributed to rapid oxidation of titanium centers at the surface of the sample, thus we could not gain any useful information about the oxidation state of titanium in these samples by this technique.

Discussion

The powder X-ray diffraction and thermogravimetric reoxidation data described in Table 1 and Figure 2 confirm that a series of phases in the compositional range $\text{Na}_2\text{La}_2\text{Ti}_2\text{RuO}_{10-x}$ ($0 < x < 2$) have been prepared via the topochemical reduction of the $x = 0$ phase. Considering the relevant reduction potentials of titanium and ruthenium ($\text{Ru}^{\text{III/II}}$ $E^\circ = +0.248$ V; $\text{Ti}^{\text{III/II}}$ $E^\circ = -0.9$ V)^{7,8}, the

most likely transition-metal oxidation state combination for the $x = 2$ phase is $\text{Na}_2\text{La}_2\text{Ti}^{\text{III}}\text{Ru}^{\text{II}}\text{O}_8$ – a combination supported by magnetization data as discussed in detail below.

The presence of Ru^{2+} centers in an extended oxide is extremely unusual. Principally this is because under the high-temperature conditions typically used to prepare extended oxides, Ru^{2+} is easily oxidized in air. Furthermore at low oxygen partial pressures, phases containing Ru^{2+} centers decompose via disproportionation to yield elemental ruthenium, and phases containing ruthenium in higher oxidation states (it should be noted it is possible to prepare a select few phases containing appreciable quantities of Ru^{3+} centers, such as $\text{LnRu}_{1-\delta}\text{O}_3$, but these typically have to be stabilized under high pressure).⁹ Thus it can be seen that phases containing Ru^{2+} are extremely metastable and can only be prepared under low-temperature, ‘kinetic’ synthesis regimes.

While topochemical reduction may appear to be an obvious route for the preparation of extended oxide phases containing low-valent ruthenium, ternary phases such as SrRuO_3 and Sr_2RuO_4 are reduced directly to elemental ruthenium and SrO , revealing the situation is more complex.^{3,4} The direct reduction of ternary ruthenates to elemental ruthenium can be attributed to the increasing thermodynamic ease of reduction of Ru centers with declining oxidation state ($\text{Ru}^{\text{III/II}}$ $E^\circ = +0.248$ V; $\text{Ru}^{\text{IV/Ru}}$; $E^\circ = +0.455$ V)⁷, thus the reducing conditions required to form Ru^{2+} centers, will readily reduce these centers further to elemental ruthenium, limiting this approach.

The first reports of the preparation of Ru^{2+} containing oxides ($\text{SrFe}_{0.5}\text{Ru}_{0.5}\text{O}_2$ and $\text{Sr}_{n+1}(\text{Fe}_{0.5}\text{Ru}_{0.5})_n\text{O}_y$)^{3,4} demonstrated that the ‘over reduction’ of Ru^{2+} to the element, can be prevented by embedding the ruthenium centers in a robust lattice which would need to be broken up in order to form elemental ruthenium. Thus the resilience of $\text{SrFe}_{0.5}\text{Ru}_{0.5}\text{O}_2$ to further

reduction can be attributed to the robustness of the Sr-Fe-O lattice in which the ruthenium is embedded. An analogous argument can be used to rationalize the stability of $\text{Na}_2\text{La}_2\text{Ti}_2\text{RuO}_{10-x}$ phases. In this instance however the La-Na-Ti-O lattice appears to be even more robust than the Sr-Fe-O framework, allowing $\text{Na}_2\text{La}_2\text{Ti}_2\text{RuO}_{10-x}$ phases to resist decomposition at temperatures in excess of 1000 °C, and allowing the preparation of materials in which the average ruthenium oxidation state spans the range from Ru^{4+} to Ru^{2+} .

If we consider the $\text{Na}_2\text{La}_2\text{Ti}_2\text{RuO}_{10-x}$ system as electronically ‘ionic’, with no significant interaction between the electronic states of the titanium and ruthenium, the preferential reduction of ruthenium rather than titanium suggests a $\text{Ru}^{\text{IV}}/\text{Ti}^{\text{IV}} - \text{Ru}^{\text{III}}/\text{Ti}^{\text{IV}} - \text{Ru}^{\text{II}}/\text{Ti}^{\text{IV}} - \text{Ru}^{\text{II}}/\text{Ti}^{\text{III}}$ sequence of transition metal oxidation states as the level of reduction of $\text{Na}_2\text{La}_2\text{Ti}_2\text{RuO}_{10-x}$ phases is increased (increasing x). The physical data collected from $\text{Na}_2\text{La}_2\text{Ti}_2\text{RuO}_{10-x}$ phases appear at first sight to broadly support this ‘ionic’ view point.

Transport data collected from $\text{Na}_2\text{La}_2\text{Ti}_2\text{RuO}_{10-x}$ phases indicate semiconducting or insulating behavior for all samples in the range $0 < x < 2$, with temperature dependent measurements indicating a VRH type mechanism, consistent with small polaron conductivity. As shown in Figure 5, the resistivity of samples at 300 K drops by over an order of magnitude on the initial reduction of $\text{Na}_2\text{La}_2\text{Ti}_2\text{RuO}_{10-x}$ and then remains at this lower value in the range $0.5 < x < 1$ before rising steeply across the $1 < x < 2$ range. These observations suggest that the dominant charge transport mechanism in the $0 < x < 1$ samples is intervalent charge hopping between $\text{Ru}^{4+/3+}$ ($0 < x < 0.5$) and then between $\text{Ru}^{3+/2+}$ ($0.5 < x < 1$). Once all the ruthenium centers are divalent at $x > 1$ the analogous intervalent charge hopping of $\text{Ti}^{4+/3+}$ has a much higher activation energy, as indicated by the large rise in resistivity at this point.

In common with the transport data, magnetization data collected from $\text{Na}_2\text{La}_2\text{Ti}_2\text{RuO}_{10-x}$ samples show a rapid change with increasing x , from the spin-glass behavior of the $x = 0$ phase, to weak paramagnetism in the range $0.5 < x < 1$, and finally almost temperature independent behavior for phases with $x \geq 1$. This decline in magnetization with increasing x in the range $0 < x < 1$ is consistent with the expected behavior on reduction from Ru^{4+} to Ru^{3+} and then Ru^{2+} . If the transition metal-centers retain a 6- or 5-fold coordination, as described above, then Ru^{4+} will adopt an $S = 1$ spin state, Ru^{3+} an $S = 1/2$ spin state and Ru^{2+} a diamagnetic $S = 0$ spin state leading to a decline to zero in the observed magnetization across the $0 < x < 1$ range. The observed magnetization of the $x = 0.51$ and $x = 0.90$ samples (Table 2) is a little smaller than would be predicted, if Ru^{3+} was acting as a simple $S = 1/2$ center – this effect has also been observed for the Ru^{3+} centers in $\text{LnRu}_{1-\delta}\text{O}_3$ phases.

A puzzling feature of the magnetization data, is the weak, temperature independent magnetization of $\text{Na}_2\text{La}_2\text{Ti}_2\text{RuO}_{10-x}$ phases in the range $1 < x < 2$. The transport data described above show phases in this compositional range are highly insulating, indicating that the electrons in titanium d-states are localized, not itinerant. We would therefore expect the magnetization of these samples to increase with increasing x as the concentration of localized $S = 1/2$, Ti^{3+} centers increases, but this is not observed. The lack of a strong paramagnetic signal from samples with $x > 1$ suggests that the electrons added to the titanium centers on reduction are ‘spin-paired’ in some way.

There are a number of mixed-valent $\text{Ti}^{3+/4+}$ oxides which show similar diamagnetic insulating behavior at low temperature, most notably phases in the $\text{Ti}_n\text{O}_{2n-1}$ series, such as Ti_3O_5 or Ti_4O_7 .¹⁰⁻
¹² In these phases the electrons in titanium d-states are localized within a Ti-Ti local bonding network in which charge localized Ti^{3+} centers form metal-metal bonds, accounting for both the

insulating and diamagnetic behavior of the materials. We propose a similar electron localization mechanism is present in $\text{Na}_2\text{La}_2\text{Ti}_2\text{RuO}_{10-x}$ ($1 < x < 2$) phases as it provides the most plausible explanation for the combination of insulating and weak paramagnetic behavior observed for these compounds.

Some support for this Ti-Ti bonding proposal is provided by the lattice parameters of the reduced phases. While the unit cell volume of $\text{Na}_2\text{La}_2\text{Ti}_2\text{RuO}_{10-x}$ phases generally declines on reduction across the whole compositional range, the a lattice parameter expands in the range where ruthenium is being reduced ($0 < x < \sim 1$) and declines in the range where titanium is being reduced ($\sim 1 < x < 2$) as shown in Table 1. These changes are consistent with the initial filling of ruthenium non-bonding/antibonding states, leading to an expansion of the lattice, followed by the filling of titanium bonding states, leading to a contraction of the lattice due to Ti-Ti bond formation. The a lattice parameter should be particularly sensitive to the formation of Ti-Ti links as the preferential location of ruthenium within the central layer of octahedra⁵ means the majority of Ti-Ti nearest neighbor vectors lie in the ab -plane.

On heating, Ti_3O_5 and Ti_4O_7 undergo transitions, at ~ 450 K and ~ 140 K respectively, to recover charge delocalized, metallic behavior.¹⁰⁻¹² Attempts to observe similar transitions in $\text{Na}_2\text{La}_2\text{Ti}_2\text{RuO}_{10-x}$ ($1 < x < 2$) phases were limited by our apparatus and the chemical reactivity of samples, however no change in resistivity consistent with the onset of metallic behavior was observed up to 370K.

While the physical data described above can be broadly accounted for by the sequential reduction of ruthenium and then titanium, XPS data collected from reduced samples show that this sequential ‘ionic’ view is not a perfect description of the $\text{Na}_2\text{La}_2\text{RuTiO}_{10-x}$ system. It can be seen in Figure 5 that the binding energy of the Ru $3d_{5/2}$ state decreases with increasing oxygen

deficiency over the entire $0 < x < 2$ range. While the rate of decrease is steeper in the $0 < x < 1$ range, the binding energy continues to get smaller in the range $1 < x < 2$, indicating that the average oxidation state of ruthenium continues to decline over the whole compositional range. This behavior is inconsistent with the strict sequential reduction of Ru^{4+} to Ru^{2+} prior to the reduction of titanium (which would lead to a plateauing of the Ru $3d_{5/2}$ binding energy for $x > 1$) and suggests a mixing of the ruthenium and titanium valence orbitals in the $\text{Na}_2\text{La}_2\text{RuTiO}_{10-x}$ system.

A further indication that the electronic states of titanium and ruthenium are mixed in $\text{Na}_2\text{La}_2\text{RuTiO}_{10-x}$ phases can be gleaned by observing that the all-titanium phase $\text{Na}_2\text{La}_2\text{Ti}_3\text{O}_{10}$ is not reduced at all, even under the most aggressive conditions used to prepare $\text{Na}_2\text{La}_2\text{RuTiO}_{10-x}$ phases (950 °C, 5% H_2/N_2), yet the titanium centers in mixed Ti/Ru phases are reduced under these conditions, indicating the presence of ruthenium modifies the reduction behavior of the titanium centers, consistent with the mixing of the electronic states of the two metals.

Conclusion

Topochemical reduction of $\text{Na}_2\text{La}_2\text{Ti}_2\text{RuO}_{10}$ demonstrates that the robust La-Na-Ti-O lattice can stabilize Ru^{2+} with respect to further reduction, allowing this highly unusual oxidation state to be maintained within an extended oxide lattice. This suggests that other robust lattices constructed from early transition metal ions (Nb^{5+} , Ta^{5+} , W^{6+} etc.) could also act as host structures to stabilize 4d and 5d transition metals in intermediate oxidation states (M^{1+} , M^{2+}) during analogous topochemical reduction reactions, by the same mechanism. In this particular instance the reduction of $\text{Na}_2\text{La}_2\text{Ti}_2\text{RuO}_{10}$ maintains 6-fold (octahedral) or 5-fold (square-based pyramid) local ruthenium coordination, leading to a diamagnetic, $S = 0$ state for the d^6 Ru^{2+} centers – the first time this state has been observed in an extended oxide phase.

FIGURES

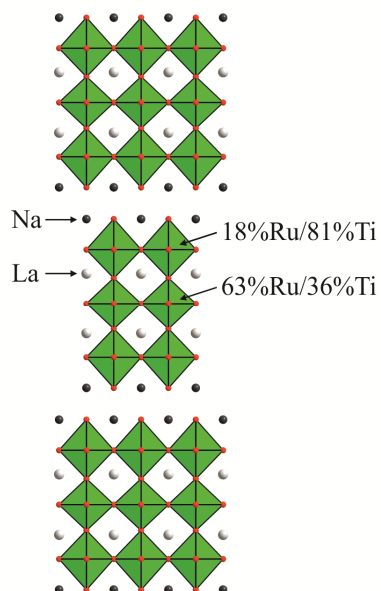


Figure 1. The crystal structure of $\text{Na}_2\text{La}_2\text{Ti}_2\text{RuO}_{10}$.

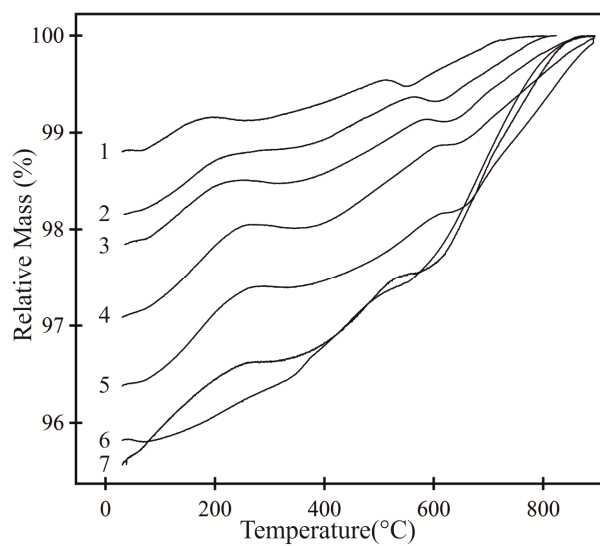


Figure 2. Thermogravimetric reoxidation data collected under oxygen from $\text{Na}_2\text{La}_2\text{Ti}_2\text{RuO}_{10}$ samples reduced by heating under 5% H_2 / 95% N_2 for 6h at 1: 400 °C, 2: 500 °C, 3: 600 °C, 4: 800 °C, 5: 900 °C, 6: 24 h at 900 °C and 7: 72 h at 900 °C.

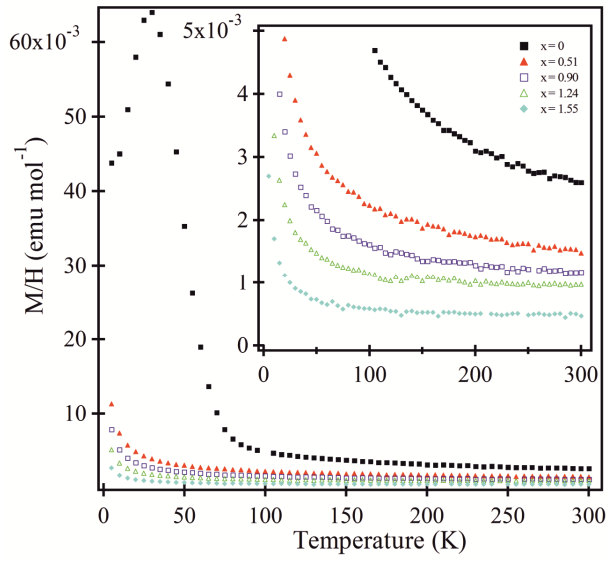


Figure 3. Zero-field cooled magnetization data collected from $\text{Na}_2\text{La}_2\text{Ti}_2\text{RuO}_{10-x}$ samples in an applied field of 100 Oe.

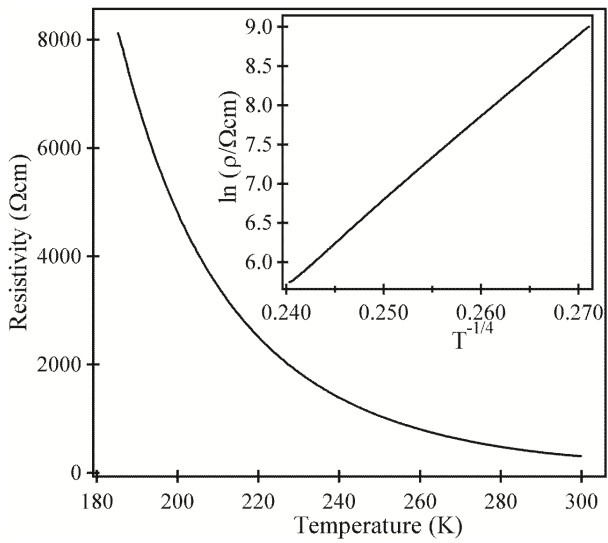


Figure 4. Resistivity of $\text{Na}_2\text{La}_2\text{Ti}_2\text{RuO}_{9.23}$ as a function of temperature. Inset shows plot of $\ln \rho$ against $T^{-1/4}$ consistent with three-dimensional variable-range hopping.

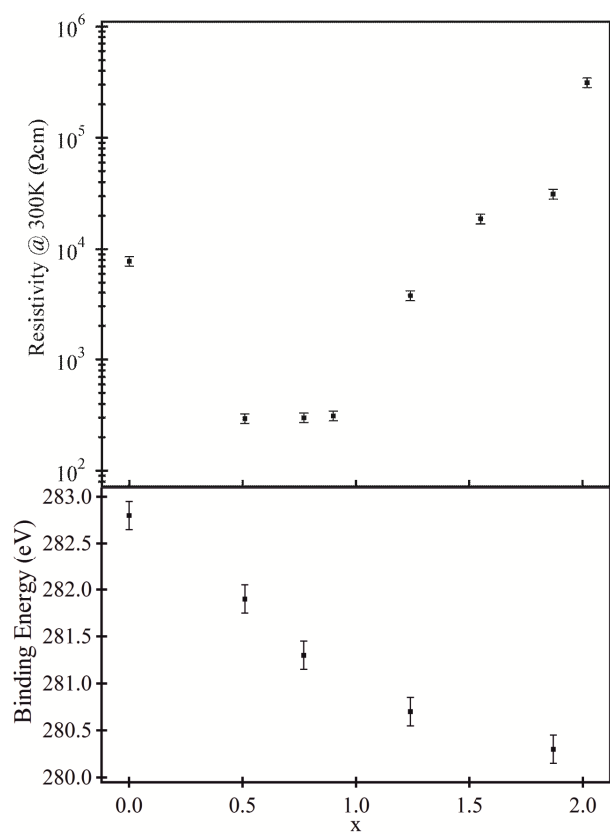


Figure 5. Plot of room temperature resistivity (top) and Ru 3d_{5/2} binding energy (bottom) as a function of oxygen deficiency for $\text{Na}_2\text{La}_2\text{Ti}_2\text{RuO}_{10-x}$ samples.

TABLES.

Temp (°C)	Time	Composition	a (Å)	c (Å)
		$\text{Na}_2\text{La}_2\text{Ti}_2\text{RuO}_{10}$	3.8594(1)	28.369(1)
300	6 hours	$\text{Na}_2\text{La}_2\text{Ti}_2\text{RuO}_{9.90(2)}$	3.8679(1)	28.212(1)
400	6 hours	$\text{Na}_2\text{La}_2\text{Ti}_2\text{RuO}_{9.49(2)}$	3.8729(1)	28.106(1)
500	6 hours	$\text{Na}_2\text{La}_2\text{Ti}_2\text{RuO}_{9.23(2)}$	3.8728(1)	28.077(1)
600	6 hours	$\text{Na}_2\text{La}_2\text{Ti}_2\text{RuO}_{9.10(2)}$	3.8737(2)	28.076(2)
800	6 hours	$\text{Na}_2\text{La}_2\text{Ti}_2\text{RuO}_{8.76(2)}$	3.8793(1)	28.032(1)
900	6 hours	$\text{Na}_2\text{La}_2\text{Ti}_2\text{RuO}_{8.45(2)}$	3.8738(1)	28.066(1)
900	24 hours	$\text{Na}_2\text{La}_2\text{Ti}_2\text{RuO}_{8.13(2)}$	3.8643(3)	28.152(2)
900	72 hours	$\text{Na}_2\text{La}_2\text{Ti}_2\text{RuO}_{7.98(2)}$	3.8637(3)	28.175(4)

Table 1. Preparation conditions, compositions and lattice parameters of $\text{Na}_2\text{La}_2\text{Ti}_2\text{RuO}_{10-x}$ samples.

x	Fit range (K)	C ($\text{cm}^3 \text{ K mol}^{-1}$)	Equivalent number of $S = 1/2$ centers (mol)	Θ (K)	K ($\text{cm}^3 \text{ mol}^{-1}$)
0	150 - 300	0.367(1)		-6.48(2)	0.00130(1)
0.51	5 - 150	0.077(1)	0.205	-2.99(3)	0.00148(2)
0.90	5 - 150	0.053(1)	0.141	-2.89(3)	0.00108(1)
1.24	5 - 150	0.031(1)	0.082	-2.32(3)	0.00084(1)
1.55	5 - 150	0.015(1)	0.040	-1.65(2)	0.00042(1)

Table 2. Parameters extracted from fitting magnetization data collected from $\text{Na}_2\text{La}_2\text{Ti}_2\text{RuO}_{10-x}$ samples to the Curie-Weiss law ($\chi = C/(T - \theta) + K$).

ASSOCIATED CONTENT

Supporting Information. Full details of the structural refinement of $\text{Na}_2\text{La}_2\text{Ti}_2\text{O}_{10-x}$ phases against X-ray powder diffraction data. Details of the XPS data collected from selected $\text{Na}_2\text{La}_2\text{Ti}_2\text{O}_{10-x}$ phases.

AUTHOR INFORMATION

Corresponding Author

* Tel : +44 1865 272623. Fax: +44 1865 272690. email: michael.hayward@chem.ox.ac.uk

Author Contributions

The manuscript was written through contributions of all authors. All authors have given approval to the final version of the manuscript.

REFERENCES

- (1) Goodenough, J. B.; Zhou, J.-S. *Chem. Mater.* **1998**, *10*, 2980
- (2) Kobayashi, K. L.; Kimura, T.; Sawada, H.; Terakura, K.; Tokura, Y. *Nature* **1998**, *395*, 677.
- (3) Denis Romero, F.; Burr, S. J.; McGrady, J. E.; Gianolio, D.; Cibir, G.; Hayward, M. A. *J. Am. Chem. Soc.* **2013**, *135*, 1838.
- (4) Denis Romero, F.; Gianolio, D.; Cibir, G.; Bingham, P. A.; d'Hollander, J.-C.; Forder, S. D.; Hayward, M. A. *Inorg. Chem.* **2013**, *52*, 10920.
- (5) Lalena, J. N.; Falster, A. U.; Simmons, W. B.; Carpenter, E. E.; Wiggins, J.; Hariharan, S.; Wiley, J. B. *Chem. Mater.* **2000**, *12*, 2418.

- (6) Wright, A. J.; Greaves, C. *J. Mater. Chem.* **1996**, *6*, 1823.
- (7) Greenwood, N. N.; Earnshaw, A. *Chemistry of the Elements*; Pergamon Press: Oxford, 1997.
- (8) We note that while the use of solution phase reduction potentials is not strictly applicable to solid-state reactions information relating to solution phase equilibria are the only data available and are sufficiently relevant to give a qualitative explanation to the observed chemical behavior.
- (9) Sinclair, A.; Rodgers, J. A.; Topping, C. V.; Misek, M.; Stewart, R. D.; Kockelmann, W.; Bos, J. W. G.; Attfield, J. P. *Angew. Chem., Int. Ed.* **2014**, *53*, 8343.
- (10) Marezio, M.; McWhan, D. B.; Dernier, P. D.; Remeika, J. P. *J. Solid State Chem.* **1973**, *6*, 213.
- (11) Mulay, L. N.; Danley, W. J. *J. Appl. Phys.* **1970**, *41*, 877.
- (12) Rao, C. N. R.; Ramdas, S.; Loehman, R. E.; Honig, J. M. *J. Solid State Chem.* **1971**, *3*, 83.

TOC Synopsis:

Topochemical reduction of $\text{Na}_2\text{La}_2\text{Ti}_2\text{RuO}_{10}$ with dilute hydrogen yields phases of composition $\text{Na}_2\text{La}_2\text{Ti}_2\text{RuO}_{10-x}$ ($0 < x < 2$). Magnetization data from samples with $x > 1$ show only very weak paramagnetism indicating that the Ru^{2+} centers present adopt $S = 0$ diamagnetic configurations (the first time this has been reported in an extended oxide) while the electrons added on the reduction of titanium are paired within a local Ti-Ti bonding network.

TOC Figure:

